Bioorganic Chemistry 50 (2013) 11–16

Contents lists available at ScienceDirect

Bioorganic Chemistry

journal homepage: www.elsevier.com/locate/bioorg

# Structural and diffusion properties of formamide/water mixture interacting with $TiO_2$ surface

E. Dushanov [a,b], Kh. Kholmurodov [a,c,*], K. Yasuoka [d]

[a] Laboratory of Radiation Biology, JINR, 141980 Dubna, Moscow Region, Russia
[b] Institute of Nuclear Physics, 702132 Ulugbek, Tashkent, Uzbekistan
[c] Dubna International University, 141980 Dubna, Moscow Region, Russia
[d] Department of Mechanical Engineering, Keio University, Yokohama 223-8522, Japan

ARTICLE INFO

*Article history:*
Received 14 February 2013
Available online 23 July 2013

*Keywords:*
Formamide molecule
Water
Surface
Catalysts
Molecular structures

ABSTRACT

The photoreaction and adsorption properties on surfaces, thermal decomposition, chemical transformation, and other properties of the formamide molecule are widely used to understand the origins of the formation of biological molecules (nucleosides, amino acids, DNA, monolayers, etc.) needed for life. The titanium oxide ($TiO_2$) surface can act both as a template on which the accumulation of adsorbed molecules like formamide occurs through the concentration effect, and as a catalytic material that lowers the activation energy needed for the formation of intermediate products. In this paper, a formamide–water solution interacting with $TiO_2$ (anatase) surface is simulated using the molecular dynamics method. The structural, diffusion and density properties of formamide–water mixture on $TiO_2$ are established for a wide temperature range from $T = 250$ K up to $T = 400$ K.



## 1. Introduction

Formamide contains the four elements (C, H, O, and N) most required for life and it is attractive as a potential prebiotic starting material for nucleobase synthesis. In the presence of catalysts (for example, $TiO_2$) and with moderate heating, formamide can pass surface energy barriers, yielding a complete set of nucleic bases and acyclonucleosides, and favoring both phosphorylations and transphosphorylations necessary for life. In the reaction mechanism, interaction with water seems to be an essential factor for the formamide molecule to function [1–5]. An important type of nucleoside base synthesis can be supposed to take place under UV light in the formamide reaction with a $TiO_2$ surface, which would underlie the crucial biological significance of this mineral in making compounds of life. In the dark conditions, the experimental data on formamide adsorption at 300 K over the (001) plane of $TiO_2$ indicate some amount of unreacted formamide and water among the products (CO, $H_2$, $NH_3$, HCN). Thus, some concentration of water and its involvement in formamide–$TiO_2$ interaction was experimentally shown to be an important constituent. Besides nucleoside synthesis, formamide actively influences *in situ* the hybridization of nucleotide, DNA, and RNA molecules [1–8].

Formamide ($CH_3NO$, hereinafter also as FM), also known as methanamide, is an amide derived from formic acid. It is a clear liquid which is miscible with water and has an ammonia-like odor. When heated strongly, FM decomposes to hydrogen cyanide (HCN) and water vapor. As a constituent, FM is also used for the cryopreservation of tissues and organs. In relation to the DNA and RNA molecules, some important formamide's properties can be outlined as follows. It stabilises RNA in gel electrophoresis by deionizing RNA; in capillary electrophoresis, it is used for stabilizing single strands of denatured DNA. FM lowers the melting point of nucleic acids, so the strands separate more readily [6]. Theoretical investigations of the chemical transformations of FM, a molecule of prebiotic interest as a precursor for biomolecules, are conducted concerning the formation of small molecules including CO, $NH_3$, $H_2O$, HCN, HNC, $H_2$, HNCO, and HOCN [9].

The solvent, dehydration, adsorption, and decomposition properties of formamide on various surfaces were intensively studied in recent experimental papers [1,2,10–13]. Some of these experimental results are summarized and descripted in [14]. In [15], it is shown for the first time that guanine, adenine, and hypoxanthine can be produced from formamide in a single model prebiotic reaction at lower temperatures than previously reported if FM is subjected to UV irradiation during heating; this observation relaxes the requirements for prebiotic purine nucleobase formation.

The aim of this work is to simulate the formamide–water (FM–W) interaction process on a $TiO_2$ (anatase) surface and to estimate the possible activation energy barrier with the molecular dynamics method. Molecular modeling was performed for the temperature range of $T = 250$ K to $T = 400$ K, and the diffusion and density profiles were established for the formamide (FM)

* Corresponding author at: Laboratory of Radiation Biology, JINR, 141980 Dubna, Moscow Region, Russia. Fax: +7 4962165948.
*E-mail address:* mirzo@jinr.ru (Kh. Kholmurodov).

0045-2068/$ - see front matter © 2013 Elsevier Inc. All rights reserved.
http://dx.doi.org/10.1016/j.bioorg.2013.07.002

and water (W) molecules on the anatase surface. In this regard, metal surfaces are often used in the synthesis and degradation of oxygen-containing compounds, such as alcohols, where carbon–carbon (C–C) and carbon–oxygen (C–O) bond formation and breakage are the elementary steps in this type of process, and the metal surface plays the primary role in the efficiency and selectivity of these steps [16].

Apart from experimental research, recent theoretical and simulation studies were mostly focused on the FM–W reaction process. Several modern theoretical and molecular dynamics (MD) studies of FM–W interactions should be mentioned in this respect [17,18]. Nevertheless, to our best knowledge, little is known about the FM–$TiO_2$ surface interaction, and almost nothing has been reported on the FM–W–$TiO_2$ one. In this paper, using the MD simulation method, we aimed to make the first attempts to investigate the FM–$TiO_2$ surface interaction mechanism in detail on the atomic/molecular level. In the presence of water (W), we elucidate the structural, diffusional, and molecular concentration distribution effects. We consider water presence to be a stabilizing factor on the FM–$TiO_2$ surface interaction mechanism.

## 2. Systems and methodology

### 2.1. Initial configuration, molecular field topology

We have simulated two liquid systems (pure FM and FM–W mixture) interacting on the oxide $TiO_2$ surface. The configuration snapshot and schematic view of the modelled systems are illustrated on Figs. 1 and 2, respectively. The FM–W mixture contains of 50–50% molecules of each (FM) and (W) liquids. The pure FM and FM–W mixture densities vary in the interval $\rho = 0.7–1.0$ g/cm$^3$. For example, the system with pure FM has 2304 molecules, the FM–W system contains 1152 molecules of FM (formamide) and 1152 molecules of W (water). The bulk $TiO_2$ (anatase) phase was defined by the unit cell lattice vectors of the following lengths: $a_0 = b_0 = 3.785$ Å and $c_0 = 9.514$ Å. The $TiO_2$ surface is (1 1 1) in the tetragonal symmetry class; t-anatase; and space group is I4(1)/amd. All the lattice parameters of surface were taken from EIM databases and dataset website supported by the Russian Foundation for Basic Research [19]. As the adsorbing surface, we have composed in total four layers of 420 $TiO_2$ molecules (5040 = 1680 (Ti) + 3360 (O) atoms). The corresponding parameters of systems are shown in Table 1.

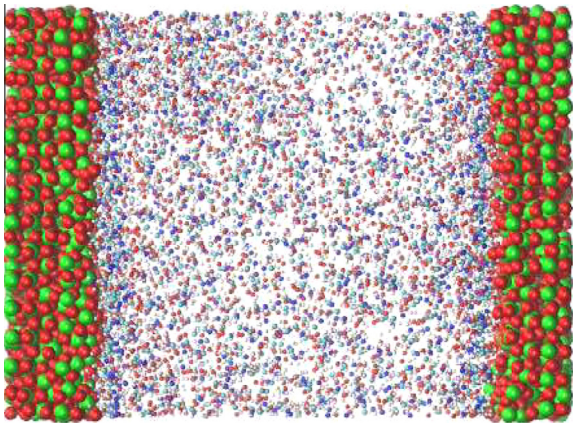

**Fig. 1.** A computer generated snapshot of FM–W mixture, relaxed inside two $TiO_2$ (anatase) wall surfaces, is shown. The green and red large balls indicate Ti and O atoms, small spheres – liquid FM–W atoms, respectively. The $TiO_2$ surface seems to be that of an amorphous solid as the thermal vibrations will slightly displace the surface atoms from their mean equilibrium positions. (For interpretation of the references to color in this figure legend, the reader is referred to the web version of this article.)

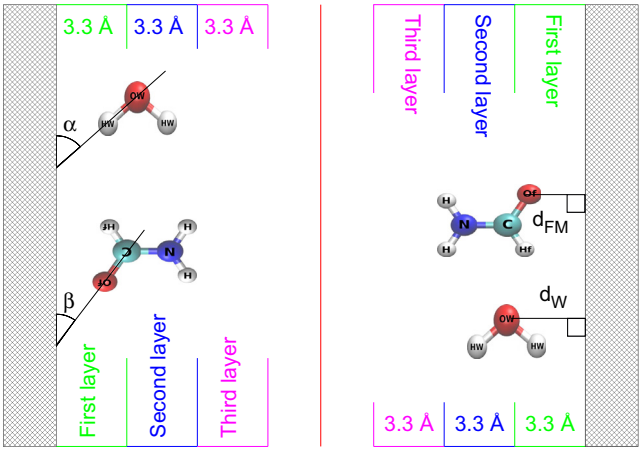


**Fig. 2.** Schematic view of model system. FM molecules are shown as C, N, Of, Hf and H sites and water molecules – as OW and HW atoms. The $\alpha$, $\beta$ identify the angles between surface and bonds in liquid (OW–HW, C–Of), respectively. The $d_W$, $d_{FM}$ indicate the minimal distances between the surface and liquid oxygen atoms.

For the modeling of intermolecular interactions we used the Lennard–Jones (LJ) potential, which commonly being applied for the description of van der Waals interactions in liquids. The LJ and electrostatics potentials look like:

$$U = \sum_{ij}\left[4\varepsilon_{ij}\left(\left(\frac{\sigma_{ij}}{r_{ij}}\right)^{12} - \left(\frac{\sigma_{ij}}{r_{ij}}\right)^{6}\right) + \frac{q_i q_j}{r_{ij}}\right] \quad (1)$$

Here $\sigma_{ij}$, $\varepsilon_{ij}$ are van der Waals interaction parameters of $i$th and $j$th atoms; $r_{ij}$ is interatomic distance; $q_i$, $q_j$ are partial atomic charges. The LJ, atomic charges and cross-interaction parameters for FM–W liquid atoms are specified on Table 5 (see, Appendix A). The cross-section interaction parameters were defined using the Lorentz–Berthelot mixing rule: $\sigma_{ij} = (\sigma_i + \sigma_j)/2$, $\varepsilon_{ij} = (\varepsilon_i \varepsilon_j)^{1/2}$.

The intramolecular interactions between the liquid molecules were descripted using the LJ potential combined with harmonic, angular and dihedral bonding potentials. For the surface atoms we used Buckingham [20] and quartic tethering interaction potentials.

The force field for the $TiO_2$ (anatase) surface was reported by Kavathekar et al. [21] and Guillot et al. [22]. For the $TiO_2$ surface models, the potential parameters were developed by Matsui and Akaogi [20].

For water, an SPC rigid body model was used [23–25]. The water bond angles and lengths were not constrained.

### 2.2. Ensemble, integration algorithm, force fields

A classical molecular dynamics study was performed using the DL_POLY_2.20 [26] general-purpose code. The NVT ensemble at $T = 300$ K in conjunction with a Nosé–Hoover thermostat with the three dimensional Ewald summation and the Verlet leapfrog scheme were employed. To calculate the long-ranged electrostatic forces, the Ewald sum with the automatic optimization parameter $f = 1.0 \times 10^{-4}$ and convergence parameter 0.24375 Å$^{-1}$ was used. The integration time step of the dynamic equations of motion was 1 fs. All simulations were periodic in three dimensions.

For the FM (formamide) and W (water) molecules, the force field parameters were choosen from the DL_FIELD database [27], which, in their turn, were taken from the CHARMM package database [28].

**Table 1**
The geometry details and molecular composition of the studied systems.

| System size | X, Å | Y, Å | Z, Å | ρ, g/cm$^3$ | Ewald parameters ($k_1$,$k_2$,$k_3$) |
|---|---|---|---|---|---|
| $(TiO_2)_{5040}(CH_3NO)_{13824}$ | 56.77 | 52.99 | 73.06 | 1.06 | 22, 22, 30 |
| $(TiO_2)_{5040}(H_2O)_{3456}(CH_3NO)_{6912}$ | 56.77 | 52.99 | 73.06 | 0.74 | 22, 22, 30 |

The detailed potential and force field topology (chemical, angular, and dihedral bond parameters, atomic charges, etc.) of FM are described below in Tables 3 and 4 of Appendix A.

A parallel Shake algorithm expressed in terms of the replicated data strategy for constraining the rigid and other chemical bonds was used [26]. The MD simulations were realized in the temperature range of 250–400 K with a step of 25 K.

## 3. Results and discussions

We generated the molecular dynamical trajectories and found the relaxed molecular configuration states for the large atomic ensembles that simulate the pure FM and FM–W mixture interacting with $TiO_2$ (anatase) surface. The FM/$TiO_2$ and FM–W/$TiO_2$ interaction processes were performed within the temperature range of $T$ = [250–400] K.

### 3.1. Z-density, dipole angle orientations and diffusion coefficients

#### 3.1.1. The density profiles and dipole angle orientations

The Z-density distribution of FM oxygen (Of) atoms, based on the atomic positions perpendicular to the $TiO_2$ surface plane are shown in Fig. 3. Fig. 3a compares the Z-densities of pure FM (dashed curve) and FM–W mixture (solid line). In Fig. 3b separately the Z-density distribution of water oxygen (OW) atoms of the FM–W mixture is presented. The results of Fig. 3a indicate that the inclusion of water to consideration substantially enhances the FM density distribution on the $TiO_2$ surface. The amplitudes of Z-densities between the FM in pure and in FM–W mixture differ more than two times. The plane atom Ti used for calculation of the minimal distances ($d_{FM}$ and $d_W$) to liquid oxygen (Of and OW) atoms. The Ti–Of distance is equal to $d_{FM}$ = 2.863 Å in absence of water and $d_{FM}$ = 2.783 Å in the presence of water. For the water on $TiO_2$ surface we have the Ti–OW minimal distance to be equal to $d_W$ = 2.383 Å.

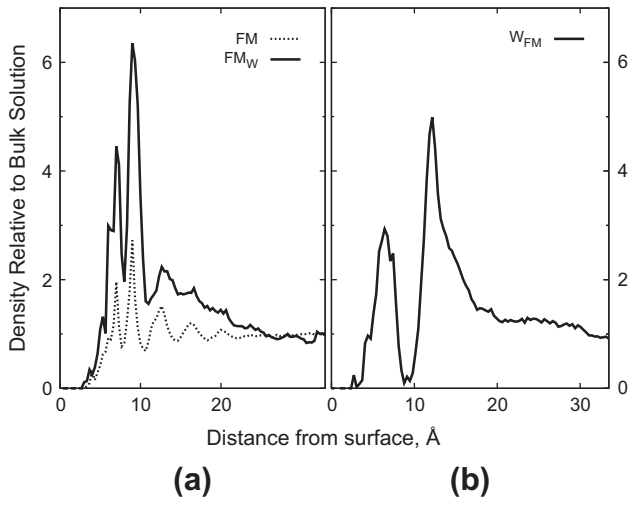


**Fig. 3.** Z-density distribution of (a) FM (formamide) and (b) W (water) molecules on $TiO_2$ surface.

**Table 2**
Dipole angle orientations on $TiO_2$ wall surfaces (%).

| Bond | Angle | | | | | | |
|---|---|---|---|---|---|---|---|
| | 60 | 70 | 80 | 90 | 100 | 110 | 120 |
| *First layer (thickness 3.3 Å, distance from surface 0 Å)* | | | | | | | |
| C–Of | | 56.5 | 43.5 | | | | |
| C–Of (W) | 09.5 | 78.0 | 12.5 | | | | |
| OW–HW | | | | | 27.5 | 52.5 | 20.0 |
| *Second layer (thickness 3.3 Å, distance from surface 3.3 Å)* | | | | | | | |
| C–Of | | | | 02.5 | 96.0 | 01.5 | |
| C–Of (W) | | | | 01.0 | 96.0 | 03.0 | |
| OW–HW | | 05.0 | 53.0 | 39.5 | 02.5 | | |
| *Third layer (thickness 3.3 Å, distance from surface 6.6 Å)* | | | | | | | |
| C–Of | | | | 05.5 | 87.0 | 07.5 | |
| C–Of (W) | | | 07.5 | 54.0 | 36.0 | 02.5 | |
| OW–HW | 01.0 | 23.5 | 66.0 | 09.0 | 0.50 | | |

Next we calculated the angles between the $TiO_2$ surface plane and liquid pair bonds C–Of of FM/$TiO_2$ and FM–W/$TiO_2$ systems. The liquid area was divided by three equal intervals, each about 3.3 Å width. The FM–W liquid layers, embedded between two $TiO_2$ wall surfaces, and the liquid bond angles, relative to the surface plane, were displayed in Fig. 2. The calculation results for dipole bond distribution are presented in Table 2.

In the first layer, for pure formamide the C–Of bonds are mostly oriented in between 70° and 80° (the percentage vary as 56.5% and 43.5%, respectively). For the formamide in water the most percentage of the C–Of (W) bonds (78%) in the first layer are oriented under 70° to the surface. At the same time, the water bonds are being oriented from 110° to 120° (compare OW–HW with C–Of and C–Of (W) in Table 2). In the second layer, the C–Of and C–Of (W) dipole angles mostly oriented under 100° to the $TiO_2$ surface plane. The amount of the bonds is 96% (Table 2). In the third layer, for pure formamide the C–Of bonds are directed under 100° (the percentage is 87%); for the formamide in water the C–Of (W) bonds are oriented between 90° and 100° (the percentage vary as 54.0% and 36.0%, respectively).

It should be stressed out that, the dipole orientation results of Table 2 have to be in a good correlation with the Z-density distributions presented above in Fig. 3. From Fig. 3a one can see that the amplitudes of the Z-densities for both pure formamide (FM) and formamide in water (FM$_W$) are located on the same distance points from the surface plane, from 6.6 Å to 9.9 Å, as the second and third layers are positioned. However, the water inclusion substantially influences both the dipole angle and Z-density distribution. The amplitude of Z-density for formamide in water is twice larger than for pure formamide, thereby resulting from the dipole angle orientations. The comparison of results in Fig. 3 and Table 2 are straightforward.

#### 3.1.2. Diffusion coefficients

From the MD simulation results, we also estimated the self-diffusion coefficient $D$ for FM and W molecules. In Fig. 4 we present the self-diffusion coefficients of FM and FM–W mixtures on $TiO_2$ surface. The temperature of the system was varied, and the temperature effect on the self-diffusion coefficient for FM and W

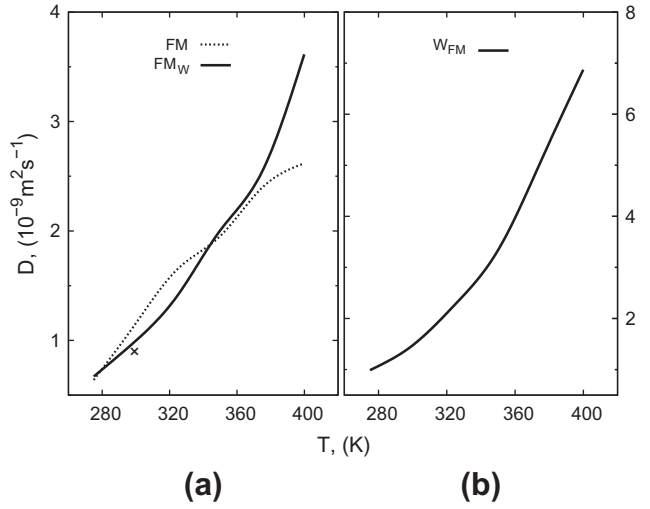


**Fig. 4.** Self-diffusion coefficients for (a) FM and FM–W mixture and (b) W as a function of temperature. The × is experimental data taken from Ref. [29,30].

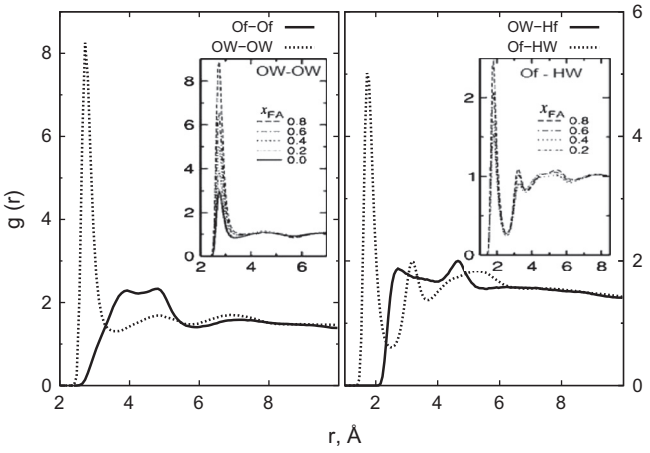


**Fig. 5.** The FM–FM, W–W and FM–W radial distribution functions (RDFs) $g(r)$ are shown. The $g(r)$ represent the Of–Of, OW–OW, Of–HW and OW–Hf atomic pair ordering. Subpictures show the RDFs for the OW–OW and Of–HW atomic pair interactions in the absence of surface taken from Ref. [30]. Note different scales on $y$ axes.

**Table 3**
The force field potentials and parameters for $TiO_2$ surface.

| $i-j$ | $A_{ij}$ (kcal mol$^{-1}$) | $\rho$ (Å) | $C_{ij}$ (kcal mol$^{-1}$ Å$^6$) |
|---|---|---|---|
| *Buckingham potential:* $A_{ij}\exp(-r_{ij}/\rho_{ij}) - C_{ij}/r_{ij}^6$ | | | |
| Ti–Ti | 717647.4 | 0.154 | 121.067 |
| Ti–O | 391049.1 | 0.194 | 290.331 |
| O–O | 271716.3 | 0.234 | 696.888 |
| $k$, kcal mol$^{-1}$/Å$^2$ | $k'$, kcal mol$^{-1}$/Å$^3$ | $k''$, kcal mol$^{-1}$/Å$^4$ | |
| *Quartic tethering potential parameters:* $kr^2/2 + k'r^3/3 + k''r^4/4$ | | | |
| 0.4 | 0.0 | 0.4 | |

molecules were estimated. It is shown that the diffusion coefficients decrease with decreasing temperature, which is consistent with the formation of longer H-bonded chains at low temperatures. Initially, at a low temperature (275 K), the presence of the surfaces had no effect on the value of $D$ for both FM and W.

The diffusion coefficient $D$, estimated for a 50:50% FM–W solution at 300 K in the presence of a $TiO_2$ (anatase) surface, was compared with experimental and other MD simulation results (by [29,30], etc). The diffusion coefficient of FM molecules $D_f$ derived from [29] was about $0.85 \times 10^{-9}$ m$^2$ s$^{-1}$ (experimental data for the FM–W mixture but without any surfaces). From our results, we have to obtain the $D_f$ value to be around $0.997 \times 10^{-9}$ m$^2$ s$^{-1}$. Thus, the presence of anatase surface re-estimates the experimental results to about 14.7% correction. At the same time, the self-diffusion coefficient of water $D_w$ are about $1.474 \times 10^{-9}$ m$^2$ s$^{-1}$ for FM–W system on anatase surface, which is also to be high than the data obtained in [30]: $1.35 \times 10^{-9}$ m$^2$ s$^{-1}$, but without surface. So far, the lack of experimental and simulation data on FM–W/$TiO_2$ system, seem to be obvious, so far our results may serve a good motivation for further experimental verification and application purposes.

### 3.2. Peculiarities of structure formations

*Liquid–surface ordering.* The structure of liquids is usually expressed in terms of radial distribution functions (RDFs) $g(r)$. The most structured and interesting $g(r)$ functions for a liquid like a FM–W solution correspond to oxygen–oxygen and oxygen–hydrogen bonding. Figs. 5 show the FM–W/$TiO_2$ structural arrangement, the peculiarities of the RDF graphs for the atomic pairs Of–Of, OW–OW, Of–HW, and OW–Hf of the formamide–water mixture. It is seen that the behavior of the RDf for water oxygen atom pair (OW–OW) is more ordered than that (Of–Of) one. The first RDF $g[OW-OW]$ peak is located at 3 Å from the zero point, which is 1.5 Å shorter than the location of the $g[Of-Of]$ RDF peak. At the same time, the Of–HW interaction is much stronger than that of OW–Hf atomic pair. The amplitude of the first $[Of-HW]$RDF peak located at 2 Å is twice higher than that of $g[OW-Hf]$, which is located around 2.8 Å.

#### 3.2.1. Comparison with experimental and MD simulation data

As it was pointed out, there is a lack of experimental and simulation data for FM–W/$TiO_2$, so we compared the MD results with some experimental and other MD data reported for the absence of the $TiO_2$ surface. In Figs. 5 the subpictures are taken from [30], where the RDFs for OW–OW and Of–HW pair interactions of the FM–W mixture were reported at the absence of surface. The comparison show that the height of RDF picks are in a good agreement with accuracy of 20%. It should be mentioned that in our FM–W system the FM amount has a $\chi \approx 0.6$ mol fraction. Thus, the inclusion of $TiO_2$ (anatase) surface from the present study has seen to essentially re-estimate the structure formation behavior of the FM–W system.

Adsorption is molecular, as the simulation approach and rigid interaction potentials used in present study imply the nondissociative liquid state. The mechanism leading to the dissociation of the water molecule is complex and induces reorganization of the surface atoms. However, as described in the literature, many metastable states (combining dissociated and nondissociated configurations) found at different water coverage are all very close in energy. Water adsorption as described in [31] can take place as chemisorption of water molecules, but without dissociation. The DFT calculations performed in [31] consider water adsorption on the (001), (100), (110), and (101) surfaces. For example, as regards the (001) surface, water is mainly dissociated; on the (100) surface, reactivity and water adsorption are thus weaker; water adsorption that occurs on the (101) surface is notably weaker than on the (100) one, and so on.

**Table 4**
The potential force field parameters for formamide molecule.

| Bond | $K$, Å kcal/mol | $r_0$, Å | Group | $K$, kcal/(mol rad$^2$) | $\theta_0$, ° | |
|---|---|---|---|---|---|---|
| Harmonic bond: $K(r_{ij}-r_0)^2/2$ | | | Angular: $K(\theta_{ijk}-\theta_0)^2/2$ | | | |
| 1–2 | 960.00 | 1.00 | 2–1–3 | 46.00 | 120.00 | |
| 1–4 | 860.00 | 1.36 | 2–1–4 | 100.00 | 120.00 | |
| 4–6 | 1300.00 | 1.23 | 1–4–6 | 150.00 | 122.00 | |
| 4–5 | 634.26 | 1.10 | 1–4–5 | 88.00 | 111.00 | |
| 1–6 | 100.00 | 2.37 | 6–4–5 | 88.00 | 122.00 | |
| 1–5 | 100.00 | 1.98 | 2–1–4 | 46.00 | 120.00 | |
| 1–3 | 960.00 | 1.00 | 3–1–4 | 100.00 | 120.00 | |
| Bond | $\varepsilon$, kcal/mol | $\sigma$, Å | Group | $K$, kcal/mol | $\delta$,° | $m$ |
| LJ parameters: $4\varepsilon((\sigma/r_{ij})^{12}-(\sigma/r_{ij})^{6})$ | | | Dihedral: $K[1+\cos(m\varphi_{ijkn}-\delta)]$ | | | |
| 2–6 | 0.0743 | 1.4473 | 2–1–4–6 | 1.40 | 180 | 2.00 |
| 2–5 | 0.0318 | 1.3760 | 2–1–4–5 | 1.40 | 180 | 2.00 |
| 3–6 | 0.0743 | 1.4473 | 3–1–4–6 | 1.40 | 180 | 2.00 |
| 3–5 | 0.0318 | 1.3760 | 3–1–4–5 | 1.40 | 180 | 2.00 |

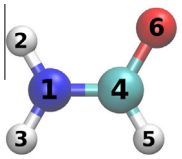


**Table 5**
The LJ, partial atomic charges and cross-interaction parameters for the liquid–surface system.

| Atom | Formamide | | | Liquid–surface | | |
|---|---|---|---|---|---|---|
| | $\varepsilon$, kcal/mol | $\sigma$, Å | $q$, a.u. | $i-j$ | $\varepsilon$, kcal/mol | $\sigma$, Å |
| N | 0.2000 | 3.2963 | −0.69 | Ti–(Of,OW) | 7.7253 | 2.3431 |
| C | 0.0700 | 3.5636 | +0.42 | Ti–C | 7.2630 | 4.1340 |
| Of | 0.1200 | 3.0291 | −0.51 | Ti–N | 0.7010 | 4.1310 |
| Hf | 0.0220 | 2.3520 | +0.08 | O–(Of,OW) | 0.2278 | 3.1306 |
| H | 0.0460 | 0.4000 | +0.35 | O–C | 0.0917 | 3.2963 |
| OW | 0.1521 | 3.1506 | −0.82 | O–N | 0.1549 | 3.1627 |

## 4. Conclusions

Based on the molecular dynamics method and using the DL_POLY_2.20 code, we simulated the FM–W interaction process on the $TiO_2$ (anatase) surface. The density distribution calculations were performed for the temperature range of $T$ = 250–400 K. For pure formamide (FM), the density profile of FM/$TiO_2$ has a weak adsorption layer between two diffuse layers. The inclusion of water in the FM–$TiO_2$ model substantially changes the density distribution profiles normal to the surface; the amplitude of the density distribution for the FM–W/$TiO_2$ surface increases. Water strongly influences the FM diffusion capabilities on the surface. At the same time, comparing the structurally important radial distribution functions, we conclude that in the FM–W/$TiO_2$ interactions the water molecules actively push formamide ones from the surface to the bulk area. Starting from the room temperatures at $T \sim 300$ K during heating and equilibration, the formamide molecules on the surface are gradually replaced by more mobile water molecules. Generated animation movies of the FM–W/$TiO_2$ interaction show that the water molecules actively push formamide ones from the surface to the bulk area. Thus, including water in the system, one can see that it significantly influences both dynamical and structural behavior of FM–W/$TiO_2$.

In the present work, we focus mostly on the nondissociative liquid state (formamide + water), interacting with a $TiO_2$ (anatase) surface. For the MD method, we use interaction potentials to simulate rigid bodies for water and formamide molecules of the liquid phase. Liquid (for example, water) adsorption on a surface is a complex phenomenon, inducing reorganization of the surface atoms. Some aspects of dissociative and nondissociative water adsorption on a $TiO_2$ (anatase) surface have been discussed in the literature [31–35].

The $TiO_2$ surface, as shown in the Fig. 1, seems to be that of an amorphous solid as the thermal vibrations will slightly displace the surface atoms from their mean equilibrium positions. Titanium dioxide is the most investigated single crystal system in the surface science of metal oxides, and the literature on anatase and rutile (110), (100), and (001) surfaces is reviewed [32]. This paper starts with a summary of a wide variety of technical fields where $TiO_2$ is important. Water adsorption may be chemisorbed (dissociative) or dissociatives. The water adsorption process was investigated in the literature for different surfaces –(001), (100), (110), and (101), although the adsorption energies at different water coverage were found to be very close to each other.

The lack of experimental and MD simulation data on the FM–W/$TiO_2$ system has been noted. Our results were compared with the experimental and other MD simulation ones, which were performed in the absence of the surface. Our study shows that the inclusion of the $TiO_2$ (anatase) surface makes it necessary to re-evaluate the structure and diffusion behavior of the FM–W system. The reported data could stimulate their further experimental verification and might be useful for application purposes.

## Acknowledgments

This work has been performed as part of a collaboration between JINR (Russia), RIKEN (Japan), and Keio University (Japan). The work has been supported in part by the Grant in Aid for the Global Center of Excellence Program to the Center for Education and Research of Symbiotic, Safe and Secure System Design from Japan's Ministry of Education, Culture, Sport, and Technology. This work was jointly supported by the JSPS (Japan Society for the Promotion of Science) and the RFBR (Russian Foundation for Basic Research); Grant No. 13-04-92100. The MD simulations have been performed using computer software, hardware facilities, and cluster machines at the CICC (JINR), RICC (RIKEN), and the Yasuoka Laboratory of Keio University (Japan). The authors would like to specially thank Mr. Sergei Negovelov (JINR) for technical assistance and helpful comments.

## Appendix A. Intramolecular bonds

See Tables 3–5.

## References

[1] S.D. Senanayake, H. Idriss, Photocatalysis and the origin of life: synthesis of nucleoside bases from formamide on TiO2(001) single surfaces, Proc. Nat. Acad. Sci. USA (PNAS) 103 (5) (2006) 1194–1198.
[2] R. Saladino, C. Crestini, G. Costanzo, E. Di Mauro, Advances in the prebiotic synthesis of nucleic acids bases: implications for the origin of life, Curr. Org. Chem. 8 (15) (2004) 1425–1443.
[3] J.P. Ferris, A.R. Hill Jr., R. Liu, L.E. Orgel, Synthesis of long prebiotic oligomers on mineral surfaces, Nature 381 (6577) (1996) 59–61.

[4] J.P. Ferris, Catalysis and prebiotic RNA synthesis, Origins Life Evol. Biospheres 23 (5–6) (1993) 307–315.
[5] Claudia Huber, Günter Wächtershäuser, Peptides by activation of amino acids with CO on (Ni,Fe)s surfaces: implications for the origin of life, Science 281 (5377) (1998) 670–672.
[6] A.M. Schoffstall, E.M. Laing, Equilibration of nucleotide derivatives in formamide, Origins Life Evol. Biospheres 14 (1–4) (1984) 221–228.
[7] A.M. Schoffstall, R.J. Barto, D.L. Ramos, Nucleoside and deoxynucleoside phosphorylation in formamide solutions, Origins Life Evol. Biospheres 12 (2) (1982) 143–151.
[8] A. Berndt, H. Kosmehl, D. Celeda, D. Katenkamp, Reduced formamide content and hybridization temperature results in increased non-radioactive mrna in situ hybridization signals, Acta Histochem. 98 (1) (1996) 79–87.
[9] V.S. Nguyen, H.L. Abbott, M.M. Dawley, T.M. Orlando, J. Leszczynski, M.T. Nguyen, Theoretical study of formamide decomposition pathways, J. Phys. Chem. A 115 (5) (2011) 841–851.
[10] V.K. Kamineni, Y.M. Lvov, T.A. Dobbins, Layer-by-layer nanoassembly of polyelectrolytes using formamide as the working medium, Langmuir 23 (14) (2007) 7423–7427.
[11] J.E. Parmeter, U. Schwalke, W.H. Weinberg, Interaction of formamide with the ru(001) surface, J. Am. Chem. Soc. 110 (1) (1988) 53–62.
[12] J.M.R. Muir, H. Idriss, Formamide reactions on rutile $TiO_2$(011) surface, Surface Sci. 603 (19) (2009) 2986–29900.
[13] R. Saladino, U. Ciambecchini, C. Crestini, G. Costanzo, R. Negri, E. Di Mauro, One-pot $TiO_2$-catalyzed synthesis of nucleic bases and acyclonucleosides from formamide: implications for the origin of life, ChemBioChem 4 (6) (2003) 514–521.
[14] R. Saladino, C. Crestini, F. Ciciriello, G. Costanzo, E. DiMauro, Formamide chemistry and the origin of informational polymers, Chem. Biodivers. 4 (4) (2007) 694–720.
[15] H.L. Barks, R. Buckley, G.A. Grieves, E. Di Mauro, N.V. Hud, T.M. Orlando, Guanine, adenine, and hypoxanthine production in UV-irradiated formamide solutions: relaxation of the requirements for prebiotic purine nucleobase formation, ChemBioChem 11 (9) (2010) 1240–1243.
[16] W.M.H. Sachtler, M. Ichikawa, Catalytic site requirements for elementary steps in syngas conversion to oxygenates over promoted rhodium, J. Phys. Chem. 90 (20) (1986) 4752–4758.
[17] S. Chalmet, M.F. Ruiz-López, Molecular dynamics simulation of formamide in water using density functional theory and classical potentials, J. Chem. Phys. 111 (3) (1999) 1117.
[18] M.H.H. Pomata, D. Laria, M.S. Skaf, M.D. Elola, Molecular dynamics simulations of AOT-water/formamide reverse micelles: structural and dynamical properties, J. Chem. Phys. 129 (24) (2008) 244503.
[19] WWW-MINCRYST. Crystallographic and Crystallochemical Database for Minerals and their Structural Analogues, 2012. <http://database.iem.ac.ru/mincryst/>.
[20] M. Matsui, M. Akaogi, Molecular dynamics simulation of the structural and physical properties of the four polymorphs of $TiO_2$, Mol. Simulat. 6 (4–6) (1991) 239–244.
[21] R.S. Kavathekar, P. Dev, N.J. English, J.M.D. MacElroy, Molecular dynamics study of water in contact with the $TiO_2$ rutile-110, 100, 101, 001 and anatase-101, 001 surface, Mol. Phys. 109 (13) (2011) 1649–1656.
[22] B. Guillot, N. Sator, A computer simulation study of natural silicate melts. Part I: Low pressure properties, Geochim. Cosmochim. Acta 71 (5) (2007) 1249–1265.
[23] H.J.C. Berendsen, J.R. Grigera, T.P. Straatsma, The missing term in effective pair potentials, J. Phys. Chem. 91 (1987) 6269–6271.
[24] G.W. Robinson, S. Singh, S.-B. Zhu, M.W. Evans, Water in biology, chemistry and physics: experimental overviews and computational methodologies, World Sci. Ser. Contemp. Chem. Phys. 9 (1996) 528.
[25] P.G. Kusalik, I.M. Svishchev, The spatial structure in liquid water, Science 265 (1994) 1219–1221.
[26] T.R. Forester, W. Smith, DlPOLY2.0: a general-purpose parallel molecular dynamics simulation package, J. Mol. Graph. 14 (3) (1996) 136–141.
[27] C.W. Yong, DL_FIELD—a force field and model development tool for DL_POLY. In: Richard Blake (Ed.), CSE Frontiers. STFCs Computational Science and Engineering Department (CSED), Number 2010, Science and Technology Facilities Council, STFC Daresbury Laboratory, October 2010, pp. 38–40.
[28] B.R. Brooks, C.L. Brooks III, A.D. Mackerell Jr., L. Nilsson, R.J. Petrella, B. Roux, Y. Won, G. Archontis, C. Bartels, S. Boresch, A. Caflisch, L. Caves, Q. Cui, A.R. Dinner, M. Feig, S. Fischer, J. Gao, M. Hodoscek, W. Im, K. Kuczera, T. Lazaridis, J. Ma, V. Ovchinnikov, E. Paci, R.W. Pastor, C.B. Post, J.Z. Pu, M. Schaefer, B. Tidor, R.M. Venable, H.L. Woodcock, X. Wu, W. Yang, D.M. York, M. Karplus, CHARMM: the biomolecular simulation program, J. Comput. Chem. 30 (10) (2009) 1545–1614.
[29] C.K. Finter, H.G. Hertz, Nmr relaxation study of I- and Na+ solvation structure in formamide (FA) and preferential solvation of these ions in the mixture FA/$H_2O$, Z. Phys. Chem. 148 (1) (1986) 75–96.
[30] M.D. Elola, B.M. Ladanyi, Computational study of structural and dynamical properties of formamide-water mixtures, J. Chem. Phys. 125 (184506) (2006) 13.
[31] C. Arrouvel, M. Digne, M. Breysse, H. Toulhoat, P. Raybaud, Effects of morphology on surface hydroxyl concentration: a DFT comparison of anatase-$TiO_2$ and -alumina catalytic supports, J. Catal. 222 (1) (2004) 152–166.
[32] U. Diebold, The surface science of titanium dioxide, Surface Sci. Rep. 48 (5–8) (2003) 53–229.
[33] C. Chizallet, M. Digne, C. Arrouvel, P. Raybaud, F. Delbecq, G. Costentin, M. Che, P. Sautet, H. Toulhoat, Insights into the geometry, stability and vibrational properties of OH groups on $\gamma$-$Al_2O_3$, $TiO_2$-Anatase and MgO from DFT calculations, Top. Catal. 52 (8) (2009) 1005–1016.
[34] C. Arrouvel, H. Toulhoat, M. Breysse, P. Raybaud, Effects of $PH_2O$, $PH_2S$, $PH_2$ on the surface properties of anatase-$TiO_2$ and $\gamma$-$Al_2O_3$: a DFT study, J. Catal. 226 (2) (2004) 260–272.
[35] A. Hémeryck, A. Motta, J. Swiatowska, C. Pereira-Nabais, P. Marcus, D. Costa, Diaminoethane adsorption and water substitution on hydrated $TiO_2$: a thermochemical study based on first-principles calculations, Phys. Chem. Chem. Phys. 15 (2013) 10824–10834.